Charge Transport in Conjugated Aromatic Molecular Junctions: Molecular Conjugation and Molecule−Electrode Coupling

Revital Cohen,[†] Kurt Stokbro,[‡] Jan M. L. Martin,[§] and Mark A. Ratner*[,†]

Department of Chemistry, Northwestern University, Evanston, Illinois 60208, Nano-Science Center, Niels Bohr Institute, Universitetsparken 5d, DK-2100 Copenhagen, Denmark, Atomistix A/S, Juliane Maries Vej 30, DK-2100 Copenhagen, Denmark, and Department of Organic Chemistry, Weizmann Institute of Science, Rehovot 76100, Israel

Received: June 12, 2007

The conductance of a single molecule transport junction is investigated in the Landauer-Imry regime of coherent tunneling transport. Utilizing aromatic systems with thiol end groups, we have calculated using density functional theory the expected conductance of junctions containing molecules with different levels of conjugation and of different lengths. The calculated variations in transport junction conductance are explained in terms of the continuity of the conjugation path between leads. Molecular conjugation describes this continuity within the molecule, and the interfacial terms (spectral densities or imaginary parts of the self-energy) describe its continuity at the molecule/metal interface. We compare the results from junction conductance calculations with isolated molecule electronic structure calculations These density functional theory calculations suggest that for these dithiol molecules, transport occurs mostly through the occupied orbital manifold. The decay of the transport with length is found to be exponential for poly-Ph dithiol molecules. We compare the calculated conductance of conjugated aromatic molecules with their molecular orbital calculations and with the Green's function formulation and evaluate the relative significance of different factors (such as energetic alignment and spectral density) that control the conductance of molecules.

Introduction

Exploring the use of individual molecules as active components in electronic devices is at the forefront of current nanoelectronics research.[1] Molecule-based devices have shown interesting features such as molecular wire behavior, switching, rectification, optical response, bistability, and mechanistic change depending on the structure.[2−10]

Because of important early measurements,[11−13] *p*-benzene dithiol (PDT) has become a prototypical case for examining transport in such junctions. Thiolated molecules on gold surfaces comprise the majority of studied devices.[14−19] These junctions are relatively stable for reasonable measurement times and are more likely to be formed reproducibly because of the strong Au−S interaction.

Aromatic compounds are of special interest in molecular transport. Their smaller highest occupied molecular orbital−lowest unoccupied molecular orbital (HOMO−LUMO) gap and functionalization capability make them attractive for potential molecular electronics applications. Many research groups have tried to understand alkane thiol/Au junction behavior,[4,7,16,17,20−31] but systematic studies of aromatic thiols describing their general structure/function behavior are fewer.[20,32−37]

The nonequilibrium Green's function/density functional theory (NEGF-DFT) approach has now become standard and is utilized extensively to describe the behavior of different molecular junctions.[7,38−53] The detailed contact structure can be influenced by many uncontrollable experimental factors and stochastic events, producing data which cannot be precisely reproduced.[54−58] Using NEGF-DFT, we have shown[21] that the conductance of a molecule is highly sensitive to geometry and can change by factors from roughly 2 to a few orders of magnitude, depending on the interface structure. The latter depends on the molecular component, the electrode type, and the quality of the electrode surface (resulting from different fabrication techniques). It is difficult to predict the behavior of one molecule on a surface if the interface structure is unknown.[59] Moreover, the molecular device structure under nonequilibrium conditions remains undefined. Thus, it appears useful to study systematically series of molecules and to compare their conductance behavior to elucidate trends in their intrinsic properties.

The conductance of a molecular junction results from interplay among several factors. In the incoherent regime, these include charge injection, leading to the generation of charge carriers on the molecular wire, and charge transport along the wire.[60−65] In the coherent regime, it is difficult to separate these factors since charge does not physically reside on the molecule. Factors such as the energy gap for injection, the spectral density coupling molecule and electrode, and the molecular electronic structure combine to determine the conductance. In this regime, it is instructive to describe the conductance of a molecular junction in terms of the continuity of the conduction pathway. The conduction pathway for coherent motion of charge is comprised of three segments: the intramolecular segment and the two molecule−electrode interface ones. To achieve efficient conductance, strong electronic coupling among the three segments should be achieved. Such coupling is provided by close energetic lineup of the molecular states with the electrode Fermi energy (small injection gap) and by substantial orbital overlap

* To whom correspondence should be addressed. E-mail: ratner@chem.northwestern.edu.
[†] Northwestern University.
[‡] Niels Bohr Institute and Atomistix A/S.
[§] Weizmann Institute of Science.

10.1021/jp0795309 CCC: $37.00
Published on Web 09/14/2007

between the structural units within the molecule (conjugation) and between the molecule and the electrodes (spectral density). Lower conductance can result from obstacles in the coherent charge propagation pathway, for example, broken conjugation or lack of strong electronic coupling at the molecule−electrode interface.[35,66] The degree of orbital overlap at the molecule−electrode interface depends both on the structure of the interface and on the orbital density distribution on the molecular contact atoms. While the interface structure may fluctuate significantly depending on the device and the experimental conditions, the orbital density on the end groups is an intrinsic feature of a molecule that does not depend on the device, experimental conditions, or interfacial structure.

The extent of the coupling at the interface can be obtained from the Green's function of the system. The low-voltage molecular junction conductance, g, depends quadratically on the Green's function according to

$$g(E) \propto \Gamma_1\Gamma_N |\, G_{1N}{}^r(E)\,|^2 \tag{1}$$

where Γ_1 and Γ_N are the spectral densities (broadening) at the two electrodes, respectively, and together with the retarded Green's function, $G_{1N}{}^r$, contain all the relevant information needed to determine the conductance. In a simple orbital presentation[67] for the wide band limit, the qualitative dependence of Green's function element between atomic orbital i (perhaps on the left sulfur) and orbital j (perhaps on the right sulfur) is given by the approximate result

$$G_{ij}{}^r(E) \approx \sum_\mu \frac{C_{i\mu}C_{j\mu}}{E - \epsilon_\mu - i\Gamma_\mu} \tag{2}$$

where $C_{i\mu}$ and $C_{j\mu}$ are the molecular orbital (MO) coefficients of atomic orbital (AO) i in MO μ, e_μ is the MO energy eigenvalue, and Γ_μ is the broadening of the MO because of electrode coupling. In the gap (where the measured and calculated conductance occurs), $|G_{ij}{}^r|^2$ may be dominated by the term

$$|G_{ij}{}^r(E)|_{\text{eff}}{}^2 \approx \frac{C_{i\mu}{}^2 C_{j\mu}{}^2}{(E - \epsilon_\mu)^2 + \Gamma_\mu{}^2} \tag{3}$$

for the μ frontier molecular orbital. Thus, the factors that account for the conductance of a molecule, the energetic alignment of the molecule and the electrode, and the interface overlap combine to determine the value of $|G_{ij}|_{\text{eff}}{}^2$. The energy gap factor is taken into account in the denominator of $|G_{ij}|_{\text{eff}}{}^2$, and the density at the molecule−electrode interface is considered in the numerator. For good conduction, $|G_{ij}|_{\text{eff}}{}^2$ should be large, requiring either $\epsilon_\mu \sim E$ (near resonance injection) or a large $C_{i\mu}C_{j\mu}$ orbital coefficient on the end groups (interface overlap) or both. Accordingly, the energy gap term $(E - \epsilon_\mu)^{-2}$ will permit significant contribution to the value of $|G_{ij}|_{\text{eff}}{}^2$ only around the Fermi energy, for example, for the frontier molecular orbitals. While the energy gap usually follows closely the molecular conjugation level (smaller gap for molecules with extended conjugation), the magnitude of the orbital coefficients on the end groups is less straightforward to predict.

Here, we report results of $I-V$ calculations and quantum chemical calculations on a series of thiolated aromatic compounds attached to Au. These results show that both the degree of conjugation[68−70] and the orbital density on the molecular end groups are key factors in achieving higher conductance because of continuous charge propagation through the junction.

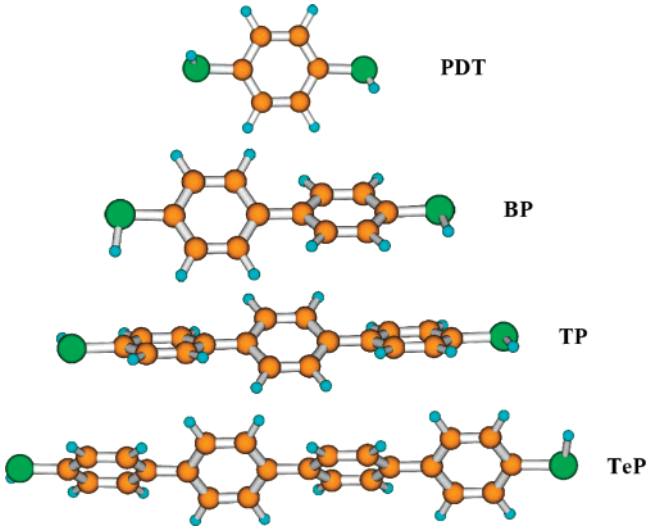

Figure 1. The isolated molecule structures of polyphenyls as optimized at the B3LYP/6-31G* level of theory. 1,4-Benzene dithiol (PDT), [1,1′-biphenyl]-4,4′-dithiol (BP), [1,1′:4′,1″-terphenyl]-4,4″-dithiol (TP), and [1,1′:4′,1″:4″,1‴-quaterphenyl]-4,4‴-dithiol (TeP).

Computational Approach

The nonequilibrium Green's function/density functional theory (NEGF-DFT) approach has now become standard and is utilized extensively to describe and predict the behavior of different molecular junctions.[7,38−41,43,47−53,71−73] While other approaches, including those based on the Lippman−Schwinger scattering method for the molecule itself coupled with the jellium representation of the electrodes,[74−76] on Hartree−Fock type methods,[77,78] or on analytic forms for the self-energies,[79,80] are also used, the NEGF formulation has an inherent elegance and generality, which makes it an attractive way to approach these issues. Details about the NEGF formalism with its advantages and applications to electronic transport are described elsewhere.[7,38−40,43,46−48] We used the TranSIESTA-C (TSC) program package[38,47,81] to study the transport properties of two-probe systems comprised of aromatic compounds. This program combines density functional theory (DFT) with the nonequilibrium Green's function formalism (NEGF) to simulate the electronic transport in single molecule devices under nonequilibrium conditions. In TSC, a molecule is embedded in a unit cell with periodic boundary conditions (the extended molecule). The model system for the transport calculation is comprised of three parts: the left electrode, the scattering region, and the right electrode. The extended molecule (scattering region) contains the optimized molecule together with 45 gold atoms,18 of the left (two 3 × 3 layers of Au surfaces) and 27 of the right electrode (three 3 × 3 layers). This is the unit cell, where the difference in the number of atoms of each electrode is necessary to maintain the periodicity of the system.[82] We used the LDA-PZ[83] exchange/correlation functional with the DZP basis set on the molecules and with SZP (5d,6s,6p) basis set[84] on the Au cluster of the extended molecules as implemented in TSC. The geometries of the isolated molecules were optimized in Gaussian03[85] using the B3LYP hybrid exchange/correlation functional,[86,87] with the 6-31G* basis set,[88] and were then used for the coherent transport calculations (Figure 1). Utilizing this computational scheme for the transmission coefficient and the current (limit of elastic scattering), we assume that the initial

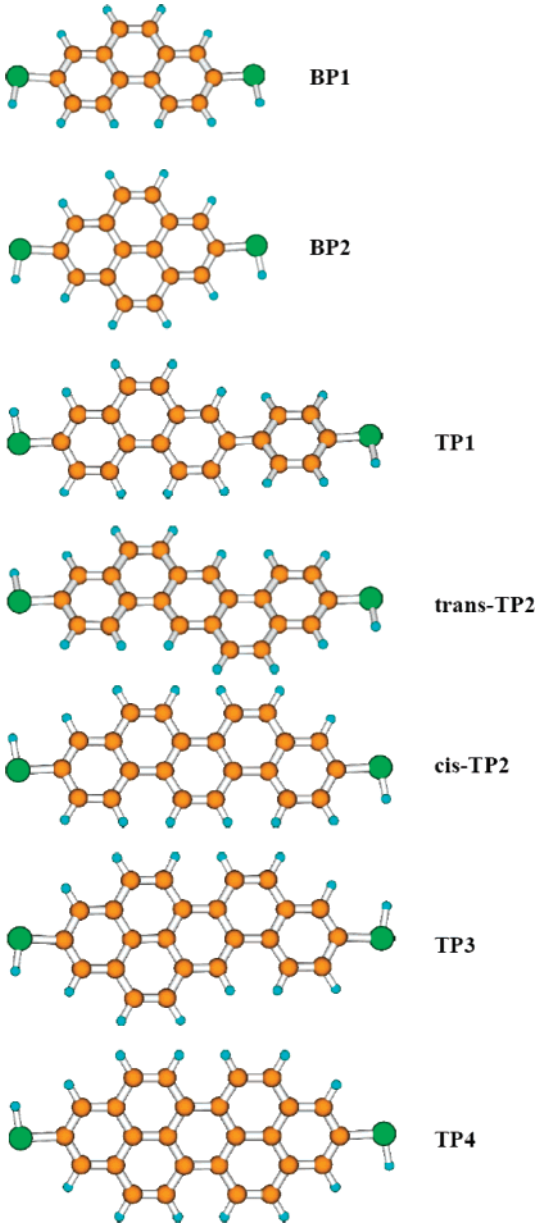

Figure 2. The isolated molecule structures of fused aromatic molecules as optimized at the B3LYP/6-31G* level of theory. Phenanthrene dithiol (BP1), pyrene dithiol (BP2), Ph-phenanthrene dithiol (TP1), dibenz-[a,h]anthracene dithiol (*trans*-TP2), picene dithiol (*cis*-TP2), naphtho-[2,1-a]pyrene dithiol (TP3), and peropyrene dithiol (TP4).

dithiol loses both hydrogen atoms upon interaction with the gold surface. The thiol ends were positioned in the FCC (threefold) site of Au(1,1,1) surface in a distance of 1.905 Å from the surface on the basis of previously reported studies of dithiol molecules in gold junctions.[21,66] Orbital coefficient values were derived from the natural population analysis (NPA)[89] calculated at the same level of theory as the geometry optimizations using Gaussian03.

Results

The *p*-benzene dithiol molecule (PDT) has already been extensively studied both experimentally and computationally by various groups using different methods.[11,26,34,43,49,66,70,73,90−112] It is mostly agreed that PDT is a hole type conductor and that the occupied orbitals responsible for the conduction have high amplitude on the sulfur atoms. Transiesta-C results (conductance of $0.6g_0$) were roughly consistent with other coherent transport

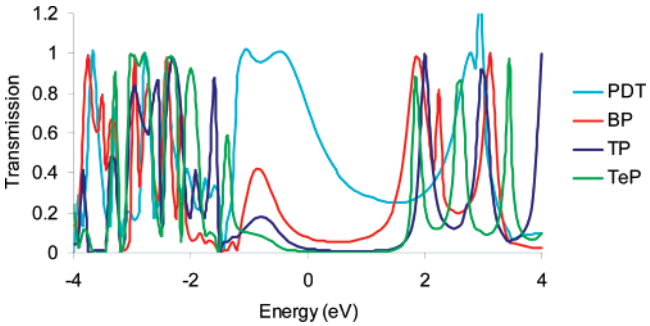

Figure 3. Equilibrium transmission versus energy characteristics of the Au/poly-Ph/Au junctions. The transmission peaks energies are relative to the metal Fermi level position, which is taken as zero.

codes (range from 10^{-2} to 5×10^{-1} g_0[34,43,73,93,113]) and agree with some of the experimental measurements describing the PDT molecule (ranging from 4×10^{-5} g_0 to 1.1×10^{-2} g_0[11,90]). These variations in both experiment and theory arise partially from assumptions regarding the crystallographic orientation of the electrodes and the bonding site, length, and angle of the molecule relative to the metal lattice; these are estimated in the theoretical calculations and cannot be verified in the experiments. We have discussed the variations in the measured conductance values of PDT in terms of structural fluctuations at the electrode−molecule interface.[21] Errors due to use of static DFT methods are almost certainly present: while DFT methods are attractive in an NEGF context, there is no persuasive theoretical argument[114,115] or decent computational demonstration that these electronic structure methods are optimal or accurate. Xiao et al.'s work[90] using electrochemical break junctions demonstrates the variation among measurements because of changes in the interfacial linkage. Because of these interfacial fluctuations and uncertainties, we focus here on a common approach from physical organic chemistry. We focus on trend changes within families of molecules, seeking mechanistic clues concerning structure/function behaviors for molecule tunneling conductance.

The extended aromatic dithiol compounds are π type conductors, whose thiol end groups contact gold electrodes similarly to PDT. However, in contrast to the planar PDT, in which the π electrons are delocalized over the entire molecule, the para-BiPh, TriPh, and TetraPh dithiol (BP, TP, and TeP, respectively) have a twisted ring configuration (Figure 1). The steric hindrance of the phenyl hydrogen atoms distorts these molecules from planarity by approximately 30 deg. This distortion decreases the conjugation by reducing the orbital overlap between the aromatic rings. Therefore, the poly-Ph molecules are not expected to be as transmissive as the PDT molecule. It has been suggested in theoretical and experimental work that the twisting of the middle benzene ring in some oligophenylene molecules greatly reduces the conductance and transfers the molecule from a conducting state to an insulating state.[116,117] Previous DFT calculations suggest that BP and TP will not transmit as well as PDT, and Xue and Ratner discussed the differences in terms of local resistivity dipoles.[34,35,118]

In contrast to the simple polyphenyl molecules shown in Figure 1, their fused aromatic analogues are planar (the isolated molecule geometries were optimized at the B3LYP/6-31G* level of theory using the G03 program package) (Figure 2). At low voltages, we expect the conduction mechanism in these molecules to be coherent tunneling, so that the species in Figure 2 should give transport junctions appropriate for the Landauer approach of eq 1.

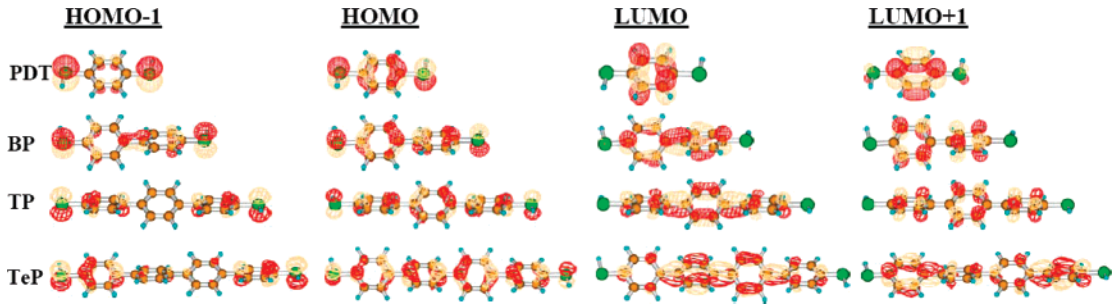

Figure 4. Frontier molecular orbital shapes of the isolated PDT, BP, TP, and TeP molecules.

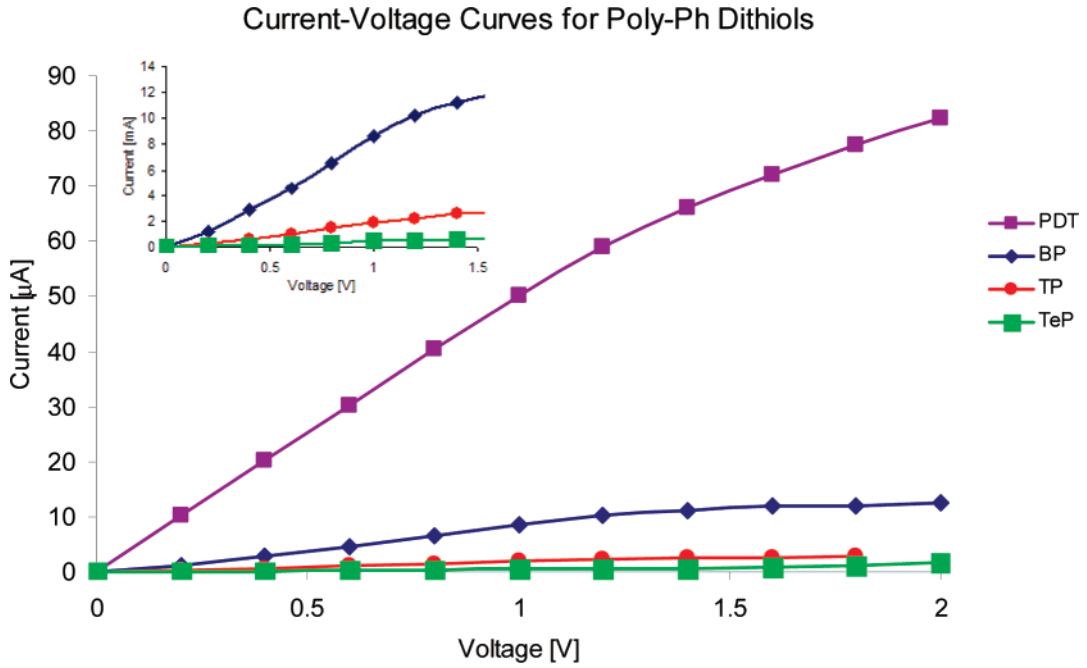

Figure 5. *I*−*V* characteristics for the poly-Ph molecules PDT, BP, TP, and TeP. The PDT was omitted for clarity in the inset, which includes the *I*−*V* characteristics for BP, TP, and TeP.

Within the *p*-BiPh dithiol family (BP, BP1, and BP2), the BP1 and BP2, which have similar length to BP, are planar and fully conjugated. One might expect them to conduct better than BP, since more extensively conjugated molecules are generally expected to have a narrower HOMO−LUMO gap; as a result, the HOMO band should be closer to the Fermi energy of the metal electrode, thus, the conduction should be higher than that for the less conjugated BP. The fully conjugated system in these molecules gives larger delocalization of the π orbitals on the carbon backbone, and thus conductance should rise from a favorable orbital overlap within the molecule (no large local resistivity dipoles[34,119]). Since all the molecules in the TriPh family (TP, TP1, cis-TP2, trans-TP2, TP3, and TP4; Figure 2) have the same length, their conductance might be expected to rise with their conjugation for the same reasons.

I. Polyaromatic Dithiols. Figure 3 shows the zero bias transmission curves for the series of polyaromatic dithiol molecules: PDT, BP, TP, and TeP. We assumed an identical interface configuration for all poly-Ph molecules since they have identical end groups.[34,35] For the four phenyl dithiol molecules studied here, we find that the metal Fermi level lines up closer to the HOMO than to the LUMO upon contact with two gold electrodes, similar to previous finding on phenyl, BiPh, and TriPh dithiol molecules.[34,35,118] Thus, the TranSIESTA-C program consistently reproduces the results of other codes (and of chemical intuition and photoemission studies[120,121]) regarding the position of the Fermi level inside the HOMO−LUMO gap.[34,35]

For PDT, strong coupling between the gold electrode and the sulfur atoms leads to a broad transmission spectrum around the Fermi energy and large zero-bias conductance because of near resonant tunneling through HOMO (Figure 3). It can be seen from Figure 3 that while the HOMO band is broad and energetically localized largely in the same place for the molecules studied, the LUMO and the LUMO + 1 bands are narrower and differ in their energy positions from molecule to molecule. This might suggest that while the HOMO is largely localized on sulfur end groups, which are common to all these molecules, the LUMO and the LUMO + 1 are mostly localized on the carbon backbone, which is different for each molecule. Additionally, the carbon backbone is coupled only slightly to the gold electrode, and thus the carbon-based LUMO and LUMO + 1 states are narrower than the thiol-based HOMO state.

Frontier orbital calculations of the isolated poly-Ph molecules (at the B3LYP/6-31G* level of theory, Figure 4) support the suggestion that the occupied orbitals are largely localized on the sulfur atoms and the unoccupied orbitals are largely localized on the carbon backbone. High orbital density on the sulfur atoms in the HOMO allows a better coupling of the molecule to the electrode resulting in a broad transmission peak (Figure 3). The

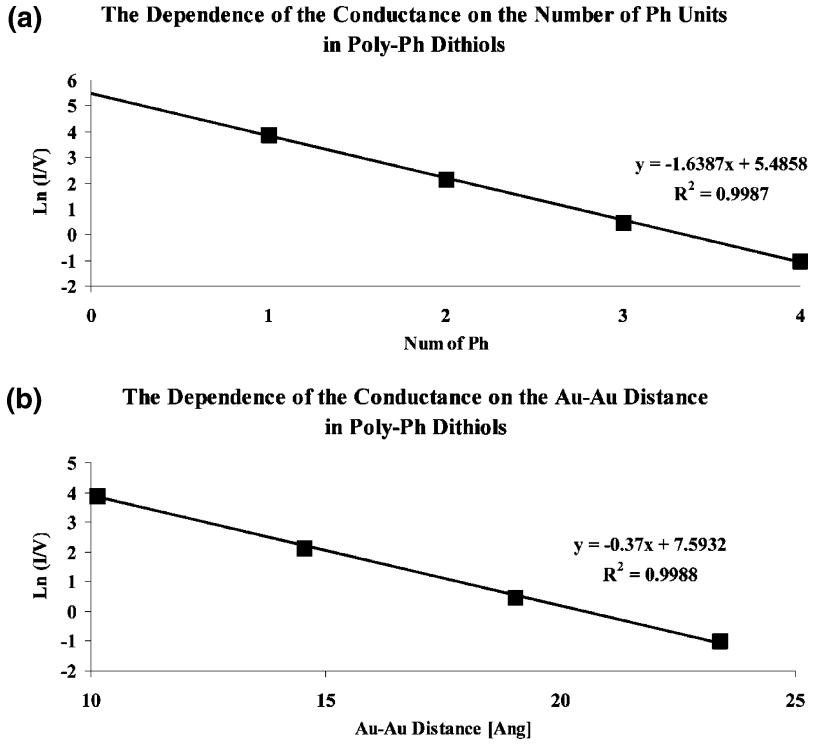

Figure 6. Linear fits for the logarithmic conductance dependence on distance for the poly-Ph molecules: PDT, BP, TP, and TeP. Conductance ($g = dI/dV$) is calculated at bias of 0.2 V. (a) Ln(g) versus the number of phenyl units, $\beta = 1.64$. (b) Ln(g) versus the distance between the gold electrodes, $\beta = 0.37$ Å^{-1}.

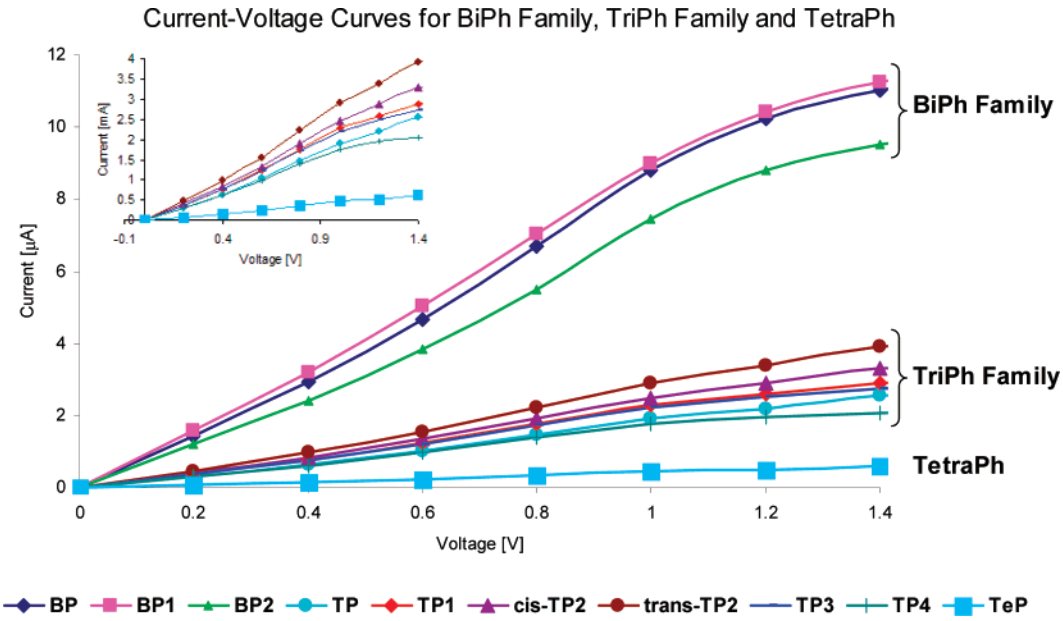

Figure 7. $I-V$ characteristics for all the computed aromatic molecules: BP, BP1, and BP2; TP, TP1, *cis*-TP2, *trans*-TP2, TP3, and TP4; and TeP. The PDT was omitted for clarity. BiPh family was omitted for clarity in the inset, which includes the $I-V$ characteristics for the TriPh family and TeP.

broadening of the peaks is a result of the imaginary part of the self-energy term, Γ, in the denominator of G_{ij} which increases with interface coupling. In contrast, low orbital density on the sulfur in the unoccupied orbitals (LUMO and LUMO + 1) results in weak coupling to the electrodes, giving narrow transmission peaks in Figure 3.

Figure 5 describes the current/voltage characterization of the poly-Ph molecules. The current is linear at low bias. The zero-bias conductance of PDT, BP, TP, and TeP molecules are 50, 6, 1.5, and 0.3 μS, respectively. These values are in reasonable agreement with other calculations reported in the literature.[35,97]

One expects the conduction of nonplanar poly-Ph to scale exponentially with length in the coherent regime. The conductance in those molecules should vary with the length, R, of poly-Ph chain as

$$g \approx \exp\{-\beta R\} \quad (4)$$

where β is the characteristic falloff parameter. The decay factor β in eq 4 depends somewhat on the metals involved and also on the nature of the interfaces. We chose low-bias voltage of 0.2 V where the current is linearly dependent on the voltage

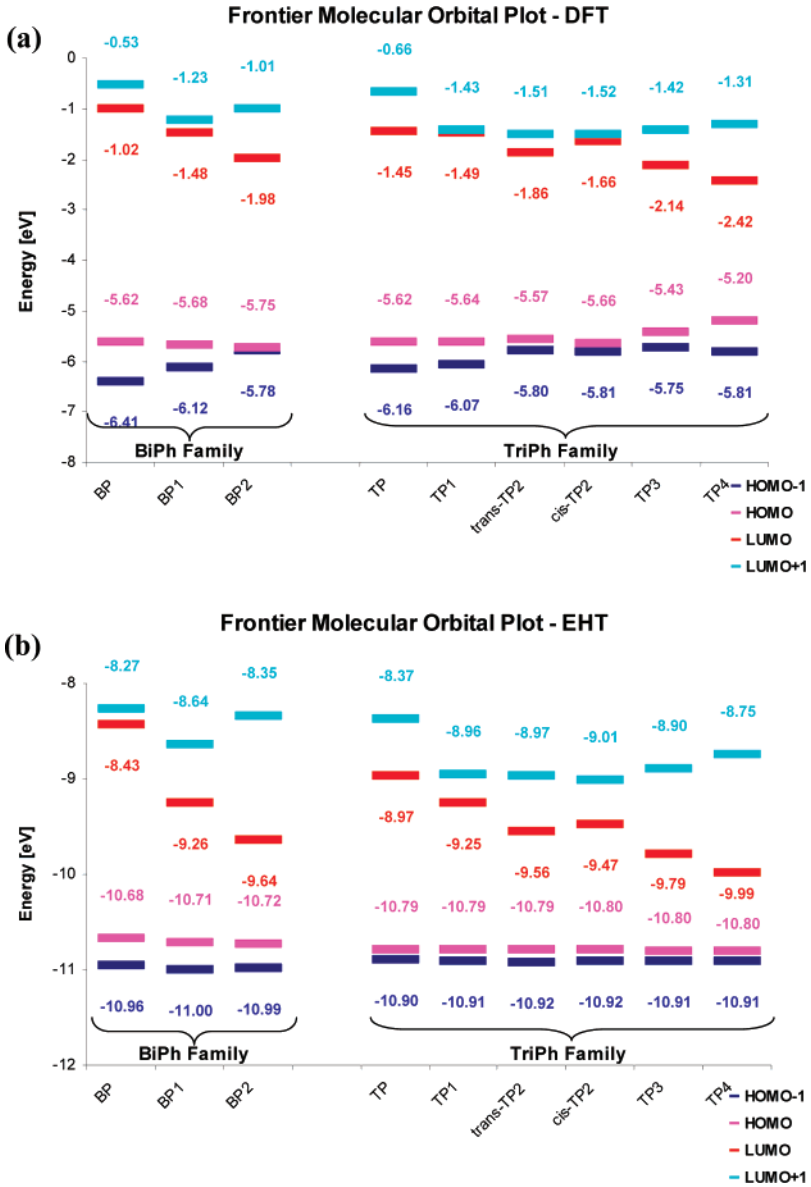

Figure 8. Frontier molecular orbital energies for the BiPh family and for the TriPh family as calculated at the (a) B3LYP/6-31G* level of theory and (b) extended Huckel theory (EHT).

and the transport mechanism is nonresonant tunneling. Figure 6 shows the distance dependence of the conductance; we obtain a β value of 1.64 as a function of number of Ph units. This translates to 0.37 $Å^{-1}$ as a function of the distance between the electrodes interfaces (Au−Au distance). The exponential decrease of the conductance with increasing number of Ph units is consistent with a nonresonance transmission through the molecule.[63] The obtained β value agrees well with those calculated and measured previously for other phenyl-based systems.[32,33,35,36,122]

II. Fused Aromatics. For each poly-Ph molecule, there is a family of "similar length/different conjugation" molecules. For example, BP1 and BP2 have essentially the same length as BP but different conjugated structure. The BP1 compound is planar and has an additional C═C bond fusing the BiPh from one side, and the BP2 molecule has two C═C bonds fusing the BiPh from both sides and forcing it to planarity (Figure 2). In the TriPh family, there are more possible fused aromatic configurations, most are planar (with the exception of TP1), and all of them have the same length as the nonplanar TP.

Figure 7 shows the calculated current voltage characteristics; the PDT was omitted for clarity. The dominant dependence of the current, which becomes evident from the separation into groups in the figure, is on the length of the compounds rather than on their internal structure. Thus, the BiPh family compounds are more conductive than the ones of the TriPh family, and TeP is the most insulating compound.

Although the differences in conductance of the molecules within each family are smaller than between the families, they are not negligible and are somewhat surprising. Focusing at the BiPh family of compounds (BP, BP1, and BP2), although the BP2 molecule is planar and the most conjugated molecule in the family, its conductance is significantly lower than for BP and BP1 (Figure 7). The latter two molecules have similar conductance although their structure is very different, with BP1 planar and BP strongly distorted.

To gain insight into these unanticipated behaviors, we have calculated the frontier molecular orbitals, the ones likely to be responsible for the transport. Figure 8 describes the energies of the frontier molecular orbitals of the BiPh and TriPh families (HOMO − 1, HOMO, LUMO, and LUMO + 1) calculated both at the B3LYP/6-31G* level of theory and at the extended Huckel theory (EHT) level. There is qualitative agreement between DFT and EHT. Thus, for the BiPh family (BP, BP1, BP2) in both

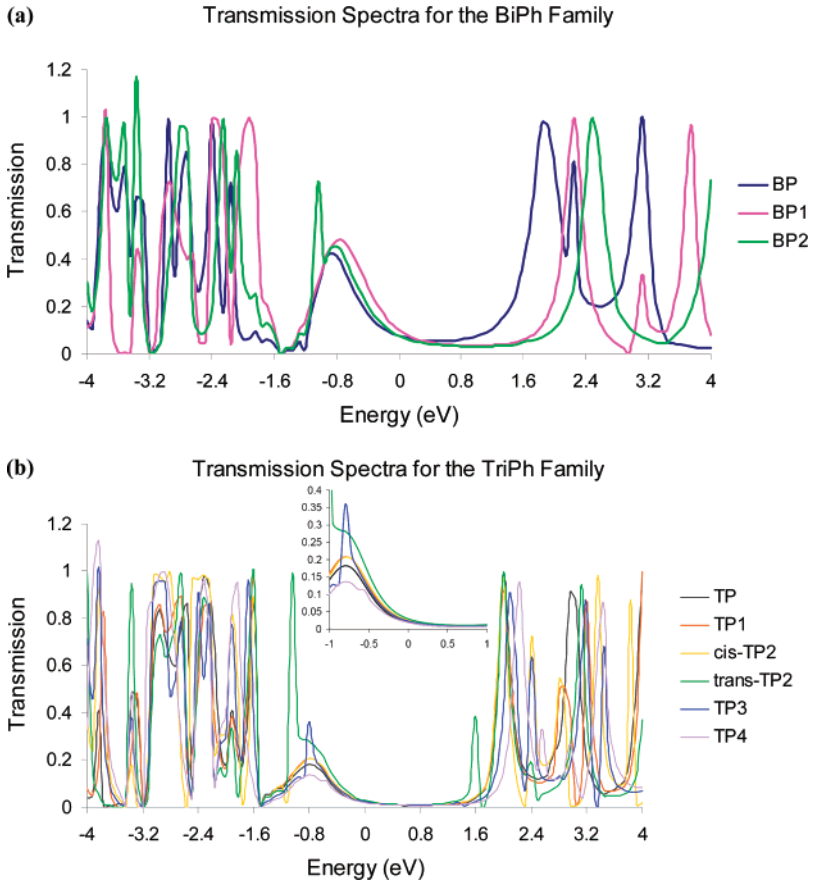

Figure 9. Equilibrium transmission versus energy characteristics of (a) Au/BiPh family/Au junctions (BP, BP1, and BP2) and (b) Au/TriPh family/Au junctions (TP, TP1, *cis*-TP2, *trans*-TP2, TP3, and TP4). The transmission peak energies are relative to the metal Fermi level position, which is taken as zero. The inset shows the enlarged transmission graphs for energy values between −1 and 1 eV (where the current is calculated).

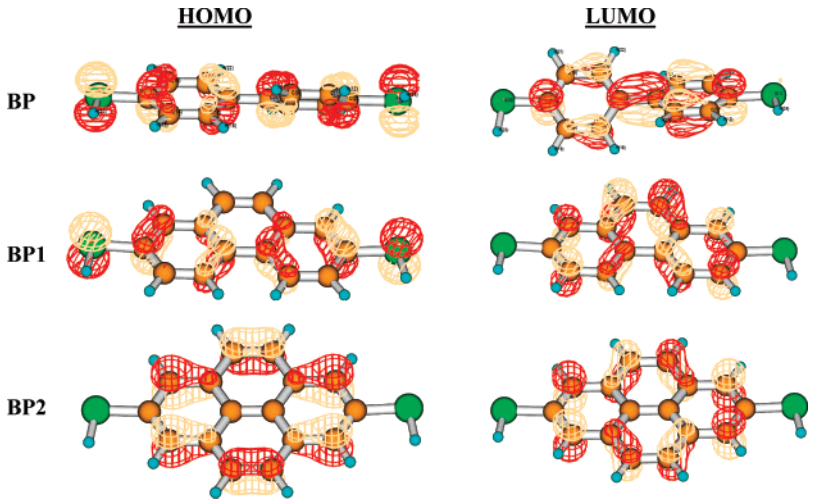

Figure 10. Frontier molecular orbital shapes of the isolated molecules of the BiPh family: BP, BP1, and BP2.

methods, the HOMO energy decreases very slightly upon increasing conjugation. The LUMO energy decreases more strongly, resulting in a decrease in the HOMO−LUMO gap with extent of conjugation, as predicted.

The same is generally true for the TriPh family of compounds (TP, TP1, trans-TP2, cis-TP2, TP3, and TP4). Once again, the HOMO−LUMO gap is smaller for more conjugated molecules (as expected), largely because of a significant drop in the LUMO energy.

The occupied orbital (HOMO) most likely dominates the conduction of the molecules (it lies closer to the Fermi energy, see Figures 9 and 3). Thus, we might expect that in each family, trends in the conductance of the molecules will be similar to the trends in the energy of the HOMO orbitals. Our results show that the changes in conductance of these molecules are varied (Figure 7): there is a small change between BP and BP1, but there is a large drop for BP2 that is not anticipated from the energetic picture: although the HOMO level of BP2 is only slightly lower than the ones of BP and BP1, its conductance[123] is considerably lower (by roughly 30%).

Figure 10 shows the calculated frontier molecular orbitals for this family. BP and BP1 have large HOMO density on the sulfur contact atoms; BP2 does not. It seems that one major factor that contributes to the large difference between the

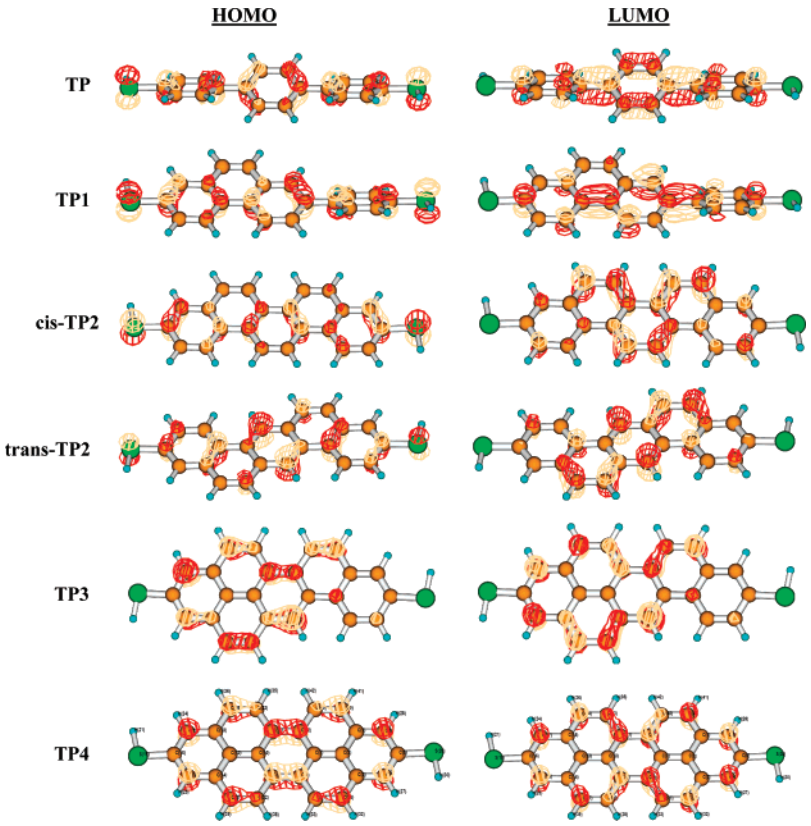

Figure 11. Frontier molecular orbital shapes of the isolated TriPh family molecules: TP, TP1, *cis*-TP2, *trans*-TP2, TP3, and TP4.

conductance of BP2 and BP or BP1 is the lack of orbital density distribution on the sulfur atoms, yielding smaller coupling and conductance for BP2. Favorable molecule−electrode coupling, required for efficient transport, is measured both by the energetic lineup of the frontier molecular orbitals with the Fermi energy of the electrode ($E - \epsilon_\mu$; eq 2) and by the effective orbital overlap at the molecule−electrode interface ($C_{i,j\mu}$; eq 2). In the BiPh family, while the injection gap ($E - \epsilon_\mu$) changes very slightly, the orbital density ($C_{i,j\mu}$ coefficients) varies significantly. With BP2, lack of orbital density on the end groups contributes to the considerable decrease in the conductance.

In the TriPh family, exactly the same discussion is valid for the lower conductance of the (more conjugated) TP3 and TP4 species (Figures 7 and 11). In the case of TP, TP1, *cis*-TP2, and *trans*-TP2, all molecules have some end-group-based HOMO density. Therefore, the trend in their relative conductance (on the basis of the $I-V$ plots, Figure 7) may follow the relative contribution of their HOMO energies and their S_{Pz} orbital coefficient values to $|G_{ij}|_{eff}^2$. In these cases, on the basis of the DFT calculations of the isolated molecules (Figure 8), both the orbital coefficients product terms and the energy gap terms combine to give smaller $|G_{ij}|_{eff}^2$ values in the order *trans*-TP2 > *cis*-TP2 > TP1 > TP, which is also the relative conductance order of the molecules calculated by Transiesta-C (Figure 7). The orbital coefficients products (numerator of $|G_{ij}|_{eff}^2$) decrease in that order, and the HOMO energies decrease to give larger energy gap (denominator of $|G_{ij}|_{eff}^2$) in the same order, resulting in lower conductance values.

Discussion and Conclusions

We have analyzed conductance of coherent molecular junctions in terms of the "continuity of the charge propagation pathway". Most previous molecular junction studies deal either with the molecular segment of the pathway (degree of coupling within the molecule)[68,124,125] by looking at the orbital delocalization over the molecular backbone or with the interface segment of the pathway (degree of coupling at the molecular junction interface) by looking at the influence of structural changes at the interface on the conductance of the junction.[21,51,70,106,110−112,126] Recent efforts to define conduction channels by diagonalizing parts of either g(E) or T(E) are promising but not yet fully persuasive.[112,127,128] We believe that the pathway continuity approach is both valid theoretically and useful for correlating transport properties with molecular characteristics.

By comparing the $I-V$ characteristics of conjugated aromatic dithiol molecules with similar length, we found that increased extent of conjugation does not necessarily lead to higher current. Availability of orbital density on the contact atoms is an important factor for high conductance values and can dominate both the conjugation of the molecule and its alignment with the electrode Fermi energy. This can be interpreted in terms of the Green's function of the system (eq 2). The G_{ij} value depends both on the energetic alignment of these orbitals with the electrodes ($E - \epsilon_\mu$) and on the interface orbital overlap (the AO coefficients $C_{i,j\mu}$ on the molecular end groups). When the conductive frontier molecular orbital (in dithiol molecules almost always the HOMO) lacks substantial orbital density on the end group, the resulting G_{ij} will drop and the conduction will be reduced considerably, even if the energetic alignment between the molecular orbitals and the electrode Fermi energy is favorable. This situation is particularly exemplified in the TriPh family. On the basis of our DFT calculations, although TP4 has the smallest energy gap (e.g., smallest denominator of $|G_{ij}|_{eff}^2$), its conductance is the lowest in the TriPh group because of small HOMO density on the end groups.[129]

In the BiPh family as well, the lack of frontier orbital density on the sulfur atoms of BP2 reduces significantly the conduction

with respect to BP1 and BP. Accordingly, our calculations suggest that BP2 and BP1 have very different conductance although they have the same length, are equally planar, and are fully conjugated.

At very small voltage, the current is proportional to the zero-voltage transmission, and then the different species (both BP and TP families) are all poorly conducting because of a substantial injection gap. With increasing voltage, the MO structure (Figure 8) along with the density on the terminal atoms (Figures 10 and 11) changes the nature of the conductance, so that BP2 is indeed less conductive than BP1 or BP and TP4 is less conductive than TP1, TP2, and TP3. This occurs as voltage is increased, because then the frontier orbital contribution clearly is more dominant than at zero voltage (because we approach a resonance with the frontier orbitals, and the Green's function is more dominated by a single level). So, the lower conductance of BP2 or TP4 is more obvious at finite than at zero voltage.

A quantitative understanding of the differences among these conductances may be obtained from a very simple barrier tunneling picture. For these single-molecule junctions, transport is due exclusively to elastic, coherent (Landauer) tunneling.[7,42,80,130,131] This is expected to drop exponentially with length, with the falloff exponent depending on conjugation and on voltage; this is seen directly (Figure 6) in our calculations. The prefactor absent from eq 4 is fixed almost entirely by the extent of mixing at the molecule/electrode interface.[4,21,132] Formally, this is clear from the Landauer-type formulas of eqs 1−5. It is this interfacial mixing variation that explains the conductance variations within families, as is clear from the isolated molecule computations (Figures 4, 10, and 11).

In summary, orbital density at the molecule−electrode interface is a significant factor to achieve high conductance values. We demonstrated this on the combination of coherent transport calculations using Transiesta-C program with quantum mechanical calculations using the G03 program.[133] Orbital density distribution is intrinsic to the molecules rather than to the junction and does not depend on the structure of the molecule−electrode interface, which may fluctuate. It is a key factor determining the conductance of molecular transport junctions, especially when comparing different molecules at the same electrode. It can therefore be used as well as the overall electrostatic potential,[34,134,135] the resistivity dipole,[34,112] and the channel analysis[119,127,128] to interpret the relative coherent conductance of transport junctions containing different molecules.

Acknowledgment. We are grateful to Professor H. Basch, Dr. Yuri A. Berlin, and Dr. Michael Galperin for helpful discussions. The research was sponsored by the NSF-MRSEC program through the Northwestern MRSEC, by the NASA URETI program, and by the NSF−NNI through the Purdue NCN Institute. We are grateful to the referees for incisive and trenchant criticism and for helpful remarks.

Supporting Information Available: Computational data on the convergence of the electrode representation (2pp). This material is available free of charge via the Internet at http://pubs.acs.org.

References and Notes

(1) Selzer, Y.; Allara, D. L. *Annu. Rev. Phys. Chem.* **2006**, *57*, 593.
(2) Carroll, R. L.; Gorman, C. B. *Angew. Chem., Int. Ed.* **2002**, *41*, 4378.
(3) James, D. K.; Tour, J. M. *Chem. Mater.* **2004**, *16*, 4423.
(4) Nitzan, A.; Ratner, M. A. *Science* **2003**, *300*, 1384.
(5) Heath, J. R.; Ratner, M. A. *Phys. Today* **2003**, 43.
(6) McCreery, R. L. *Chem. Mater.* **2004**, *16*, 4477.
(7) Nitzan, A. *Annu. Rev. Phys. Chem.* **2001**, *52*, 681.
(8) Bowler, D. R. *J. Phys.: Condens. Matter* **2004**, *16*, R721.
(9) Moore, A. M.; Dameron, A. A.; Mantooth, B. A.; Smith, R. K.; Fuchs, D. J.; Ciszek, J. W.; Maya, F.; Yao, Y. X.; Tour, J. M.; Weiss, P. S. *J. Am. Chem. Soc.* **2006**, *128*, 1959.
(10) Grill, L.; Moresco, F. *J. Phys. C* **2006**, *18*, S1887.
(11) Reed, M. A.; Zhou, C.; Muller, C. J.; Burgin, T. P.; Tour, J. M. *Science* **1997**, *278*, 252.
(12) Andres, R. P.; Bein, T.; Dorogi, M.; Feng, S.; Henderson, J. I.; Kubiak, C. P.; Mahoney, W.; Osifchin, R. G.; Reifenberger, R. *Science* **1996**, *272*, 1323.
(13) Dorogi, M.; Gomez, J.; Osifchin, R.; Andres, R. P.; Reifenberger, R. *Phys. Rev. B* **1995**, *52*, 9071.
(14) Wold, D. J.; Frisbie, C. D. *J. Am. Chem. Soc.* **2001**, *123*, 5549.
(15) Slowinski, K.; Fong, H. K. Y.; Majda, M. *J. Am. Chem. Soc.* **1999**, *121*, 7257.
(16) York, R. L.; Nguyen, P. T.; Slowinski, K. *J. Am. Chem. Soc.* **2003**, *125*, 5948.
(17) Engelkes, V. B.; Beebe, J. M.; Frisbie, C. D. *J. Am. Chem. Soc.* **2004**, *126*, 14287.
(18) Dadosh, T.; Gordin, Y.; Krahne, R.; Khivrich, I.; Mahalu, D.; Frydman, V.; Sperling, J.; Yacoby, A.; Bar-Joseph, I. *Nature* **2005**, *436*, 677.
(19) Andrews, D. Q.; Cohen, R.; Van Duyne, R. P.; Ratner, M. A. *J. Chem. Phys.* **2006**, *125*, 174718.
(20) Kaun, C.-C.; Guo, H. *Nano Lett.* **2003**, *3*, 1521.
(21) Basch, H.; Cohen, R.; Ratner, M. A. *Nano Lett.* **2005**, *5*, 1668.
(22) Jiang, J.; Lu, W.; Luo, Y. *Chem. Phys. Lett.* **2004**, *400*, 336.
(23) Wang, W.; Lee, T.; Reed, M. A. *J. Phys. Chem. B* **2004**, *108*, 18398.
(24) Holmlin, R. E.; Haag, R.; Chabinyc, M. L.; Ismagilov, R. F.; Cohen, A. E.; Terfort, A.; Rampi, M. A.; Whitesides, G. M. *J. Am. Chem. Soc.* **2001**, *123*, 5075.
(25) Cui, X. D.; Zarate, X.; Tomfohr, J.; Sankey, O. F.; Primak, A.; Moore, A. L.; Moore, T. A.; Gust, D.; Harris, G.; Lindsay, S. M. *Nanotechnology* **2002**, *13*, 5.
(26) Tomfohr, J.; Sankey, O. F. *J. Chem. Phys.* **2004**, *120*, 1542.
(27) Smalley, J. F.; Feldberg, S. W.; Chidsey, C. E. D.; Linford, M. R.; Newton, M. D.; Liu, Y. P. *J. Phys. Chem.* **1995**, *99*, 13141.
(28) Rampi, M. A.; Whitesides, G. M. *Chem. Phys. Lett.* **2002**, *281*, 373.
(29) Bumm, L. A.; Arnold, J. J.; Dunbar, T. D.; Allara, D. L.; Weiss, P. S. *J. Phys. Chem. B* **1999**, *103*, 8122.
(30) Xu, B. Q.; Tao, N. J. *Science* **2003**, *301*, 1221.
(31) Fan, F. F.; Yang, J.; Cai, L.; Price, D. W.; Dirk, S. M.; Kosynkin, D. V.; Yao, Y.; Rawlett, A. M.; Tour, J. M.; Bard, A. J. *J. Am. Chem. Soc.* **2002**, *124*, 5550.
(32) Ishida, T.; Mizutani, W.; Aya, Y.; Ogiso, H.; Sasaki, S.; Tokumoto, H. *J. Phys. Chem. B* **2002**, *106*, 5886.
(33) Wold, D. J.; Haag, R.; Rampi, M. A.; Frisbie, C. D. *J. Phys. Chem. B* **2002**, *106*, 2813.
(34) Xue, Y.; Ratner, M. A. *Phys. Rev. B* **2003**, *68*, 115406.
(35) Xue, Y.; Ratner, M. A. *Int. J. Quantum Chem.* **2005**, *102*, 911.
(36) Kaun, C.-C.; Larade, B.; Guo, H. *Phys. Rev. B* **2003**, *67*, 121411-(R).
(37) Su, W.; Jiang, J.; Luo, Y. *Chem. Phys. Lett.* **2005**, *412*, 406.
(38) Brandbyge, M.; Mozos, J.-L.; Ordejon, P.; Taylor, J.; Stokbro, K. *Phys. Rev. B* **2002**, *65*, 165401.
(39) Damle, P.; Ghosh, A. W.; Datta, S. *Chem. Phys.* **2002**, *281*, 171.
(40) Datta, S. *Superlattices Microstruct.* **2000**, *28*, 253.
(41) Datta, S. *Nanotechnology* **2004**, *15*, S433.
(42) Datta, S. *Quantum Transport: Atom to Transistor*; Cambridge University Press, 2005.
(43) Hall, L. E.; Reimers, J. R.; Hush, N. S.; Silverbrook, K. *J. Chem. Phys.* **2000**, *112*, 1510.
(44) Pecchia, A.; Latessa, L.; Di Carlo, A.; Lugli, P.; Neihaus, T. *Physica E* **2003**, *19*, 139.
(45) Shimazaki, T.; Xue, Y. Q.; Ratner, M. A.; Yamashita, K. *J. Chem. Phys.* **2006**, *124*.
(46) Stokbro, K.; Taylor, J.; Brandbyge, M.; Ordejon, P. *Ann. N.Y. Acad. Sci.* **2003**, *1006*, 212.
(47) Taylor, J.; Guo, H.; Wang, J. *Phys. Rev. B* **2001**, *63*, 245407.
(48) Xue, Y.; Datta, S.; Ratner, M. A. *Chem. Phys.* **2002**, *281*, 151.
(49) Albrecht, M.; Song, B.; Schnurpfeil, A. *J. Appl. Phys.* **2006**, *100*, 013702.
(50) Ke, S.-H.; Baranger, H. U.; Yang, W. *Phys. Rev. B* **2004**, *70*, 085410.
(51) Lawson, J. W.; Bauschlicher, J. C. W. *Phys. Rev. B* **2006**, *74*, 125401.
(52) Meunier, V.; Lu, W. C.; Sumpter, B. G.; Bernholc, J. *Int. J. Quantum Chem.* **2006**, *106*, 3334.
(53) Nakamura, H.; Yamashita, K. *J. Chem. Phys.* **2006**, *125*, 194106.

(54) Weiss, P. S. *Science* **2004**, *303*, 1136.
(55) Donhauser, Z. J.; Mantooth, B. A.; Kelly, K. F.; Bumm, L. A.; Monnell, J. D.; Stapleton, J. J.; Price, D. W., Jr.; Rawlett, A. M.; Allara, D. L.; Tour, J. M.; Weiss, P. S. *Science* **2001**, *292*, 2303.
(56) Ramachandran, G. K.; Hopson, T. J.; Rawlett, A. M.; Nagahara, L. A.; Primak, A.; Lindsay, S. M. *Science* **2003**, *300*, 1413.
(57) Wassel, R. A.; Fuierer, R. R.; Kim, H.; Gorman, C. B. *Nano Lett.* **2003**, *3*, 1617.
(58) Ulrich, J.; Esrail, D.; Pontius, W.; Venkataraman, L. *J. Phys. Chem.* **2006**, *110*, 2462.
(59) Zhirnov, V. V.; Cavin, R. K. *Nat. Mater.* **2006**, *5*, 11.
(60) Berlin, Y. A.; Burin, A. L.; Ratner, M. A. *Superlattices Microstruct.* **2000**, *28*, 241.
(61) Berlin, Y. A.; Hutchison, G. R.; Rempala, P.; Ratner, M. A.; Michl, J. *J. Phys. Chem. A* **2003**, *107*, 3970.
(62) Burin, A. L.; Ratner, M. A. *J. Polym. Sci., Part B* **2003**, *41*, 2601.
(63) Nitzan, A.; Jortner, J.; Wilkie, J.; Burin, A. L.; Ratner, M. A. *J. Phys. Chem. B* **2000**, *104*, 5661.
(64) Segal, D.; Nitzan, A.; Davis, W. B.; Wasielewski, M. R.; Ratner, M. A. *J. Phys. Chem. B* **2000**, *104*, 3817.
(65) *Introducing Molecular Electronics;* Cuniberti, G., Fagas, G., Richter, K., Eds.; Springer: New York, 2005.
(66) Samanta, M. P.; Tian, W.; Datta, S.; Henderson, J. I.; Kubiak, C. P. *Phys. Rev. B* **1996**, *53*, R7626.
(67) This is qualitatively correct only, since E and H do not generally commute, so that they are not diagonalized simultaneously. However, for this coherent transport regime, Γ is so large that eq 2 holds.
(68) Karzazi, Y.; Cornil, J.; Bredas, J. L. *J. Am. Chem. Soc.* **2001**, *123*, 10076.
(69) Seminario, J. M.; Zacarias, A. G.; Derosa, P. A. *J. Chem. Phys.* **2002**, *116*, 1671.
(70) Li, Z.-L.; Zou, B.; Wang, C.-K.; Luo, Y. *Phys. Rev. B: Condens. Matter Mater. Phys.* **2006**, *73*, 075326.
(71) Datta, S. *Electronic Transport in Mesoscopic Systems*; Cambridge University Press, 1995.
(72) Galperin, M.; Nitzan, A.; Ratner, M. A. *Phys. Rev. B* **2006**, *73*, 045314.
(73) Stokbro, K.; Taylor, J.; Brandbyge, M.; Mozos, J.-L.; Ordejon, P. *Comp. Mat. Sci.* **2003**, *27*, 151.
(74) Lang, N. D. *Phys. Rev. B* **1995**, *52*, 5335.
(75) Di Ventra, M.; Lang, N. D. *Phys. Rev. B* **2002**, *65*, 045402.
(76) Sai, N.; Zwolak, M.; Vignale, G.; Di Ventra, M. *Phys. Rev. Lett.* **2005**, *94*.
(77) Galperin, M.; Nitzan, A. *Ann. N.Y. Acad. Sci.* **2003**, *1006*, 48.
(78) Delaney, P.; Greer, J. C. *Phys. Rev. Lett.* **2004**, *93*, 036805.
(79) Remacle, F.; Levine, R. D. *J. Phys. Chem. B* **2004**, *108*, 18129.
(80) Kemp, M.; Mujica, V.; Ratner, M. A. *J. Chem. Phys.* **1994**, *101*, 5172.
(81) Taylor, J.; Brandbyge, M. M.; Stokbro, K. *Phys. Rev. Lett.* **2002**, *89*, 138301.
(82) See Transiesta-C manual for details: http:// www.atomistix.com/manuals/TranSIESTA-C-Linux.pdf. See supporting information for jusification of this number and geometry of Au atoms, as well as the basis set on Au.
(83) Perdew, J. P.; Zunger, A. *Phys. Rev. B* **1981**, *23*, 5048.
(84) Soler, J. M.; Artacho, E.; Gale, J. D.; Garcia, A.; Junquera, J.; Ordejon, P.; Sanchez-Portal, D. *J. Phys. Condens. Matter* **2002**, *14*, 2745.
(85) Pople, J. A. et al. *Gaussian 03*, Revision C.02; Gaussian, Inc.: Wallingford, CT, 2004.
(86) Becke, A. D. *J. Chem. Phys.* **1993**, *98*, 5648.
(87) Stevens, P. J.; Devlin, F. J.; Chabalowski, C. F.; Frisch, M. J. *J. Phys. Chem.* **1994**, *98*, 11623.
(88) Hay, P. J.; Wadt, W. R. *J. Chem. Phys.* **1985**, *82*, 284.
(89) Reed, A. E.; Curtiss, L. A.; Weinhold, F. *Chem. Rev.* **1988**, *88*, 899.
(90) Xiao, X. Y.; Xu, B. Q.; Tao, N. J. *Nano Lett.* **2004**, *4*, 267.
(91) Yaliraki, S. N.; Roitberg, A. E.; Gonzalez, C.; Mujica, V.; Ratner, M. A. *J. Chem. Phys.* **1999**, *111*, 6997.
(92) Wang, C.-K.; Fuc, Y.; Luo, Y. *Phys. Chem. Chem. Phys.* **2001**, *3*, 5017.
(93) Emberly, E. G.; Kirczenow, G. *Phys. Rev. B* **1998**, *58*, 10911.
(94) Di Ventra, M.; Pantelides, S. T.; Lang, N. D. *Phys. Rev. Lett.* **2000**, *84*, 979.
(95) Derosa, P. A.; Seminario, J. M. *J. Phys. Chem. B* **2001**, *105*, 471.
(96) Chen, H.; Lu, J. Q.; Wu, J.; Note, R.; Mizuseki, H.; Kawazoe, Y. *Phys. Rev. B* **2003**, *67*, 113408.
(97) Datta, S.; Tian, W. D.; Hong, S. H.; Reifenberger, R.; Henderson, J. I.; Kubiak, C. P. *Phys. Rev. Lett.* **1997**, *79*, 2530.
(98) Yaliraki, S. N.; Kemp, M.; Ratner, M. A. *J. Am. Chem. Soc.* **1999**, *121*, 3428.
(99) Kornilovitch, P. E.; Bratkovsky, A. M. *Phys. Rev. B* **2001**, *64*, 195413/1.
(100) Bratkovsky, A. M.; Kornilovitch, P. E. *Phys. Rev. B* **2003**, *67*, 115307/1.
(101) Wang, C.-K.; Luo, Y. *J. Chem. Phys.* **2003**, *119*, 4923.
(102) Nara, J.; Kino, H.; Kobayashi, N.; Tsukada, M.; Ohno, T. *Thin Solid Films* **2003**, *438*−*439*, 221.
(103) Tikhonov, A.; Coalson, R. D.; Dahnovsky, Y. *J. Chem. Phys.* **2002**, *117*, 567.
(104) Kopf, A.; Saalfrank, P. *Chem. Phys. Lett.* **2004**, *386*, 17.
(105) Lang, N. D.; Avouris, P. *Phys. Rev. B* **2001**, *64*, 125323.
(106) Basch, H.; Ratner, M. A. *J. Chem. Phys.* **2005**, *123*, 234704.
(107) Crljen, Z.; Grigoriev, A.; Wendin, G.; Stokbro, K. *Phys. Rev. B* **2005**, *71*, 165316.
(108) Benesch, C.; Cizek, M.; Thoss, M.; Domcke, W. *Chem. Phys. Lett.* **2006**, *430*, 355.
(109) Romaner, L.; Heimel, G.; Gruber, M.; Bredas, J. L.; Zojer, E. *Small* **2006**, *2*, 1468.
(110) Ke, S.-H.; Baranger, H. U.; Yang, W. *J. Am. Chem. Soc.* **2004**, *126*, 15897.
(111) Tanibayashi, S.; Tada, T.; Watanabe, S.; Yoshizawa, K. *Jpn. J. Appl. Phys.* **2005**, *44*, 7729.
(112) Grigoriev, A.; Skoldberg, J.; Wendin, G.; Crljen, Z. *Phys. Rev. B* **2006**, *74*, 045401.
(113) Di Ventra, M.; Pantelides, S. T.; Lang, N. D. *Appl. Phys. Lett.* **2000**, *76*, 3448.
(114) Muralidharan, B.; Ghosh, A. W.; Datta, S. *Phys. Rev. B* **2006**, *73*, 155410/1.
(115) Koentopp, M.; Burke, K.; Evers, F. *Phys. Rev. B* **2006**, *73*, 121403.
(116) Chen, J.; Reed, M. A.; Rawlett, A. M.; Tour, J. M. *Science* **1999**, *286*, 1550.
(117) Seminario, J. M.; Zacarias, A. G.; Derosa, P. A. *J. Phys. Chem. A* **2001**, *105*, 791.
(118) Xue, Y.; Ratner, M. A. *Phys. Rev. B* **2004**, *70*, 081404.
(119) Buttiker, M.; Martin, A. M. *Phys. Rev. B* **2000**, *61*, 2737.
(120) Zangmeister, C. D.; Robey, S. W.; Van Zee, R. D.; Yao, Y.; Tour, J. M. *J. Phys. Chem. B* **2004**, *108*, 16187.
(121) Zhu, X. Y. *Surf. Sci. Rep.* **2004**, *56*, 1.
(122) The phenyl-based systems reported earlier (ref 38) are poly-Ph methanethiols. They have a thiolated benzylic group in one end of the molecule and phenylic hydrogen in the other end; therefore, their intrinsic structure is very different and they are considerably less conductive than the dithiolated poly-Ph studied here. The fact that they have similar β values to the one we obtain in the current study suggests that the decay factor β is mostly dependent on the core structure of the molecules rather than on the end groups, the interface geometry, or the degree of orbital overlap between the end groups and the backbone of the molecule.
(123) This is clear from Figure 7, for $V > 0.4$ V.
(124) Seminario, J. M.; Zacarias, A. G.; Tour, J. M. *J. Am. Chem. Soc.* **2000**, *122*, 3015.
(125) Karzazi, Y.; Cornil, J.; Bredas, J. L. *Nanotechnology* **2003**, *14*, 165.
(126) Ke, S.-H.; Baranger, H. U.; Yang, W. *J. Chem. Phys.* **2005**, *123*, 114701.
(127) Djukic, D.; vanRuitenbeek, J. M. *Nano Lett.* **2006**, *6*, 789.
(128) Solomon, G. C.; Gagliardi, A.; Pecchia, A.; Frauenheim, T.; Di Carlo, A.; Reimers, J. R.; Hush, N. S. *Nano Lett.* **2006**, *6*, 2431.
(129) Our analysis in terms of MOs and $G\hat{}_{\mathrm{eff}}^{2}$ is qualitative rather than quantitative. Other important factors (such as the inclusion of more energy levels in G and the self-energy broadening which is not taken here into account) can alter the results in different situations. However, our qualitative treatment of the problem is convenient and straightforward as long as one knows its limitations.
(130) Landauer, R. *IBM J.* **1957**, *1*, 223.
(131) Buttiker, M.; Imry, Y.; Landauer, R.; Pinhas, S. *Phys. Rev. B* **1985**, *31*, 6207.
(132) Beebe, J. M.; Engelkes, V. B.; Miller, L. L.; Frisbie, C. D. *J. Am. Chem. Soc.* **2002**, *124*, 11268.
(133) Although use of DFT methods within the NEGF scheme is not yet a very well justified procedure, we believe that the effects calculated here are robust and will hold even if a better justified level of electronic structure modeling were to be used.
(134) Liang, G. C.; Ghosh, A. W.; Paulsson, M.; Datta, S. *Phys. Rev. B* **2004**, *69*, 115302.
(135) Mujica, V.; Roitberg, A. E.; Ratner, M. *J. Chem. Phys.* **2000**, *112*, 6834.